Tanshinone IIA ameliorates non-alcoholic fatty liver disease through targeting peroxisome proliferator-activated receptor gamma and toll-like receptor 4

Lu Huang[1,2] ⓘ, Wei Ding[3], Ming-Qiang Wang[4],
Zheng-Gen Wang[2], Hong-Hui Chen[2],
Wen Chen[2], Qiong Yang[2], Ting-Na Lu[1],
Qing Yang[1] and Ji-Man He[1,5]

Abstract

Objective: To investigate the cellular mechanisms of action of tanshinone IIA on the fatty liver disease induced by a high-fat diet in an animal model of non-alcoholic fatty liver disease (NAFLD).
Methods: Adult male Sprague Dawley rats were randomized into one of three groups: regular rat diet (CON group) for 4 months; high-fat diet (HFD group) for 4 months; HFD for 2 months followed by tanshinone IIA treatment plus HFD (TAN group) for a further 2 months. A range of physical and biochemical markers of lipid accumulation and fatty liver disease were measured and compared between the groups.
Results: Tanshinone IIA treatment significantly reduced fat accumulation in the liver and plasma lipid levels that had been increased by HFD. The toll-like receptor (TLR4)/nuclear factor kappa B (NF-κB) signalling pathway was silenced by tanshinone IIA treatment. Tumour necrosis factor-α and interleukin-6 were reduced by tanshinone IIA. Hepatocyte apoptosis was inhibited by

[1]Guangdong Provincial Key Laboratory of
Gastroenterology, Department of Gastroenterology,
Nanfang Hospital, Southern Medical University,
Guangzhou, Guangdong Province, China
[2]Department of Gastroenterology, The Second Affiliated
Hospital of University of South China, Hengyang, Hunan
Province, China
[3]Department of Urology, The First Affiliated Hospital of
Guiyang College of Traditional Chinese Medicine,
Guiyang, Guizhou Province, China

[4]Guiyang College of Traditional Chinese Medicine,
Guiyang, Guizhou Province, China
[5]Liver Research Center, Brown University,
Providence, USA

Corresponding author:
Ji-Man He, Liver Research Center, Brown University,
Providence, USA, Providence, RI 02912, USA.
Email: dr.huanglu@tom.com

tanshinone IIA. Tanshinone IIA upregulated peroxisome proliferator-activated receptor gamma (PPAR-γ), which resulted in an improvement in the oxidative status.

Conclusion: Tanshinone IIA ameliorates NAFLD by targeting PPAR-γ and TLR4, resulting in decreased plasma lipids and oxidative stress, suggesting this strategy may form the basis of novel NAFLD therapies.

Introduction

Non-alcoholic fatty liver disease (NAFLD) is a chronic liver disease with an estimated prevalence of 25% across the world, which is characterized by the accumulation of triglycerides in hepatocytes and the prevalence parallels the large-scale obesity epidemic.[1–4] Patients with NAFLD may develop non-alcoholic steatohepatitis, which is associated with hepatic necroinflammation, fibrosis, and this in turn may develop into cirrhosis, portal hypertension and hepatitis.[5,6] The pathogenesis and progression of NAFLD have not been well studied and effective licensed therapies are still in development.

The peroxisome proliferator-activated receptor gamma (*PPARG*) gene, which encodes PPAR-γ, is regulated by fatty acid and cholesterol metabolites and plays a critical role in lipid homeostasis.[7,8] The activation of PPAR-γ requires binding to peroxisome proliferator-activated receptor gamma coactivator-1 alpha (PGC-1α).[9] PPAR-γ and PGC-1α regulate mitochondrial biogenesis, cellular energy production, thermogenesis and lipid metabolism.[9] PPAR-γ has been implicated in the hepatic lipid accumulation that is important in the progression of hepatic steatosis in a high-fat diet (HFD)-induced rodent model, suggesting

that PPAR-γ may be a key molecule in the development of NAFLD.[10]

Toll-like receptors (TLRs), especially TLR4, have been shown to be associated with the pathogenesis of NAFLD by modulating the inflammatory responses via the production of inflammatory cytokines.[11] Circulating levels of lipopolysaccharide (LPS), a cellular component of gram-negative bacteria, are increased, resulting in dyslipidaemia in an HFD-induced rodent model.[11] TLR4, a receptor for LPS, which mediates innate immunity against gram-negative bacterial infections, is also upregulated in NAFLD rodents.[12,13] Activated TLR4 recruits myeloid differentiation primary response 88 (MyD88) to their intracellular domains, and subsequently recruits the death-domain-containing serine/threonine kinases, interleukin-1 receptor-associated kinase (IRAK)-1 and IRAK-4, following activation of downstream adapter protein tumour necrosis factor (TNF) receptor associated factor (TRAF)-6.[14] Traf-6 can link Tir-domain-containing receptors to IkB kinase (IKK) complex induced nuclear factor kappa B (NF-κB) activation by phosphorylation inhibitor of kB-subunit α (IkB-α) and induced degradation of IkB-αs.[15,16] TLRs can induce liver inflammation and activate

transcriptional factor NF-κB by stimulation of MyD88/IKK/IkB,[15,16] following regulation of immune and inflammatory genes.[17–19] The TLR4/NF-κB signalling pathway involved in inflammation and apoptosis is induced by LPS.[20–22] Upregulation of the TLR4/NF-κB pathway plays a key role in mediating the development of steatosis.[23,24] It has been reported that TNF-α and interleukin (IL)-6 have proinflammatory functions that are regulated through the TLR4/NK-κB pathway.[25–27] TNF-α and IL-6 are the proinflammatory cytokines that mediate fatty liver in patients with NAFLD.[28] IL-1β is generated upon caspase-1 activation, providing feed-forward stimulation for inflammatory cytokines, leading to amplification of inflammation.[29] Inflammation activation contributes to NAFLD development.[30]

Sodium tanshinone IIA sulfonate, derived from tanshinone IIA, is a water-soluble substance.[31] Tanshinone IIA is the main lipophilic component isolated from *Salvia miltiorrhiza* Bge, which is also known as the Chinese herbal medicine Danshen; and it possesses anti-atherosclerosis, anti-cardiac hypertrophy, anti-oxidant, anti-arrhythmia and anti-inflammatory properties.[32,33] Danshen is widely used to treat cardiovascular and cerebrovascular diseases following adverse treatment effects in China.[34] The effects of Danshen on other diseases such as type 2 diabetes mellitus, acute lung injury and fatty liver have been investigated.[35–37] Studies about the effects of tanshinone IIA on fatty liver, especially NAFLD, remain limited. For example, tanshinone IIA has been reported to attenuate oxidative stress and inhibit apoptosis in liver steatosis.[37] However, the cellular mechanisms of tanshinone IIA on fatty liver remain unknown. Research into how tanshinone IIA brings about changes in fatty

liver disease is urgently need. This present study investigated the cellular mechanisms of action of tanshinone IIA on fatty liver disease induced by HFD in an animal model of NAFLD in order to better understand how it may prevent fatty liver disease and to help with the future development of novel therapies for steatosis.

Materials and methods

Animals and treatments

Thirty 8-week-old male Sprague Dawley rats (approximately 300 g) were obtained from the Animal Centre of Southern Medical University, Guangzhou, China and they were cared for according to the Guiding Principles for the Animal Care and Use Committee of Southern Medical University. The rats were housed individually in an animal facility under controlled conditions (12-h light/12-h dark cycle). All studies conducted in rats were undertaken according to the Chinese Association for Laboratory Animal Sciences. The rats were randomly divided into three groups at study entry using a computer-generated randomization schedule ($n = 10$ in each group): control (CON), high-fat diet (HFD), and tanshinone IIA plus HFD (TAN) groups. All groups were given free access to food and water during the experimental period.

Rats in the HFD and TAN groups were fed a high-fat diet (1% cholesterol, 10% lard, 10% egg yolk powder and 79% standard rat chow; Zeigler Brothers, Gardner, PA, USA), while those in the CON group were fed a regular balanced diet for 4 months. During the last 2 months of the HFD diet, rats in the TAN group received sodium tanshinone IIA sulfonate as previously described.[37] Briefly, 10 mg/kg sodium tanshinone IIA sulfonate (Shanghai First Biochemical Pharmaceutical, Shanghai,

China) was intraperitoneally injected once daily, while those in the CON and HFD groups received the same quantity of normal saline for the same duration of time. Whole blood samples were obtained from the abdominal aorta under general anaesthesia and collected in heparin-containing blood tubes. Blood samples were left to stand at 37°C for 1 h and centrifugated at 3 000 *g* for 15 min at 4°C in a Sorvall[TM] Legend[TM] Micro 21R Microcentrifuge (Thermo Fisher Scientific, Rockford, IL, USA). The plasma obtained was stored at –80°C until further use. Briefly, rats were executed by cervical vertebra dislocation. After sacrifice, the livers were quickly resected, rinsed in ice-cold saline, weighed and frozen in liquid nitrogen.

RNA extraction and real-time PCR

Total RNA was extracted from 50 mg liver using a TRIzol® reagent-based protocol (Thermo Fisher Scientific), followed by quantification and quality assessment. Briefly, after samples were added to 1 ml RNAiso Plus and left to stand for 10 min at room temperature, the samples were shaken vigorously for 10 s after adding 200 µl chloroform. The samples were left to stand for 5 min at room temperature. After centrifugation at 11 000 *g* for 15 min at 4°C in a Sorvall[TM] Legend[TM] Micro 21R Microcentrifuge (Thermo Fisher Scientific), the aqueous phase was transferred to a fresh tube and mixed with the same volume of 2-propanol. After the mixture was centrifuged again at 11 000 *g* for 15 min at 4°C in a Sorvall[TM] Legend[TM] Micro 21R Microcentrifuge (Thermo Fisher Scientific), the RNA contaminated with gDNA was purified using a HiScript II 1st Strand cDNA Synthesis Kit (+gDNA wiper) (Vazyme Biotech, Nanjing, China) to remove gDNA. The qRT SuperMix II from the same kit was used to synthesize cDNA. All reactions were run in triplicate.

The cycling programme involved preliminary denaturation at 95°C for 5 min, followed by 40 cycles of denaturation at 95°C for 5 s, annealing at 60°C for 30 s, and elongation at 72°C for 30 s, followed by a final elongation step at 72°C for 5 min, and was performed on a CFX96 Touch Real-Time PCR Detection System (BioRad, Hercules, CA, USA). Polymerase chain reaction (PCR) products were separated on 1% agarose gels and visualized using ethidium bromide staining and UV light to verify the products sizes. Glyceraldehyde 3-phosphate dehydrogenase was used as the loading control for normalization of the data. Data from real-time PCR were analysed using the $2^{-\Delta\Delta Ct}$ method. The primers used for real-time PCR are listed in Table 1 and were synthesized by Sangon Biotech Company (Shanghai, China).

Western blot analysis

Total liver proteins were extracted using RIPA Lysis and Extraction Buffer (Thermo Fisher Scientific) with a complete protease inhibitor cocktail (Roche, Basel, Switzerland). Protein concentration was measured using a Pierce[TM] BCA Protein Assay Kit (Thermo Fisher Scientific 23225). Subcellular fractionation was used to isolate the nucleus as previously described.[38] Cells were collected in 10 mM phosphate-buffered saline (pH 7.4) containing 5 mM ethylenediaminetetra-acetic acid (EDTA). The cells were harvested in cytosolic lysis buffer (10 mM HEPES, 10 mM KCl, 0.1 mM EDTA, 1 mM dithiothreitol [DTT], 0.5 mM phenylmethylsulfonyl fluoride [PMSF]). After 20 min of swelling on ice, 10% Nonidet P-40 was added to the suspension, which was vortexed for 10 s and then centrifuged at 1200 *g* for 5 min at 4°C in a Sorvall[TM] Legend[TM] Micro 21R Microcentrifuge (Thermo Fisher Scientific). The resulting supernatant

Table 1. Primers sequences for real-time polymerase chain reaction.

Primer	Sequence	Size, base pairs
TLR4	Sense: 5′-TTCTAACCTCAACGACCTCACA-3′	157
	Antisense: 5′-GCCTTAGCCTCCTCTCCTTAG-3′	
PPAR-γ	Sense: 5′-CTGACCCAATGGTTGCTGATTAC-3′	80
	Antisense: 5′-GGACGCAGGCTCTACTTTGATC-3′	
Ikk	Sense: 5′-AACGCTGAAGGAAGACTGTAAC-3′	168
	Antisense: 5′-AGGTCAATCTGGATGCTGGTT-3′	
Nf-κB	Sense: 5′-ACGACACCTCTACACATAGCA-3′	145
	Antisense: 5′-CCTCATCTTCTCCAGCCTTCT-3′	
GAPDH	Sense: 5′-GTTCAACGGCACAGTCAAGG-3′	120
	Antisense: 5′-ACATACTCAGCACCAGCATCA-3′	

TLR4, toll-like receptor 4; PPAR-γ, peroxisome proliferator-activated receptor gamma; Ikk, IkB kinase; Nf-κB, nuclear factor kappa B; GAPDH, glyceraldehyde 3-phosphate dehydrogenase.

contained the cytosolic protein fraction. The nuclear pellet was resuspended in nuclear lysis buffer (20 nM HEPES, 0.4 M NaCl, 1 mM EDTA, 1 mM DTT, 0.5 mM PMSF), was mechanically lysed for 25 min and then centrifuged at 12000 g for 5 min at 4°C in a Sorvall^{TM} Legend^{TM} Micro 21R Microcentrifuge (Thermo Fisher Scientific).

Protein lysates (10 µg per lane) were electrophoresed using 10% sodium dodecyl sulphate–polyacrylamide gel electrophoresis and then transferred onto polyvinylidene fluoride membranes (Millipore, Billerica, MA, USA) using Trans-Blot® Plus electroblot apparatus at 150 mA for 1.5 h (BioRad). After blocking the membranes in 5% non-fat milk for 1 h at room temperature, they were probed with the corresponding primary antibodies overnight at 4°C for 16 h. The primary antibodies used were as follows: anti-rabbit PPAR-γ polyclonal antibodies (1:1000 dilution; bs-0530R; Bioss Antibodies, Woburn, MA, USA); anti-rabbit TLR4 polyclonal antibodies (1:1000 dilution; bs-20594R; Bioss Antibodies); anti-rabbit NF-κB polyclonal antibodies (1:500 dilution; BS-10037R; Bioss Antibodies); anti-rabbit phospho (p)-NF-κB p65 monoclonal antibody (1:1000 dilution; 3033; Cell Signaling Technology, Danvers, MA, USA); anti-rabbit PGC-1α antibodies (1:1000 dilution; 2178s; Cell Signaling Technology); anti-rabbit MyD88 monoclonal antibody (1:1000 dilution; 4283s; Cell Signaling Technology); anti-rabbit Ikk-β antibodies (1:500 dilution; AF6009; Affinity Biosciences, Cincinnati, OH, USA); anti-rabbit phospho (p)-Ikb-α monoclonal antibody (1:1000 dilution; 2859s; Cell Signaling Technology); anti-rabbit β-actin monoclonal antibody (1:1000 dilution; 8457; Cell Signaling Technology); and anti-rabbit lamin B1 monoclonal antibody (1:1000 dilution; 13435; Cell Signaling Technology). β-actin was used as the internal loading control and lamin B1 was a nuclear control. After washing with TBS-T (10 mM Tris, 150 mM NaCl, 0.05% Tween-20, pH 7.6) three times (15 min each time), membranes were then incubated with matched secondary antibodies conjugated to horseradish peroxidase (HRP) is goat anti-rabbit IgG (H+L) secondary antibody, HRP (1:10000 dilution; 31460; Thermo Fisher Scientific) for 1 h at room temperature. After washing with TBS-T (pH 7.6) three times (15 min each time), the membranes were then visualized using an enhanced chemiluminescence

reagent kit (Thermo Fisher Scientific) by film development. The blots were scanned using Canon MP Navigator EX software and a CanoScan LiDE 700F flatbed scanner (Canon, Tokyo, Japan).

Histological section preparation and staining

Paraffin-embedded liver samples were cut into 4 μm sections, deparaffinized in xylene and rehydrated through a graded series of ethanol. The tissue sections were stained with haematoxylin solution for 1 min. After differentiating the sections in 1% acid alcohol for 30 s, they were counterstained in eosin solution for 30 s. Sections were dehydrated and mounted with resin. Typical single or multiple lipid droplets within the cytoplasm of the hepatocytes was the characteristic sign of fatty liver disease. Frozen liver tissues were cut into 10 μm sections and stained with Oil Red O (Sigma-Aldrich, St Louis, MO, USA; O026) for 10 min at room temperature. All the sections were visualized and photographed using a DM4 M microscope (Leica, Solms, Germany). Lipid droplets stain red with Oil Red O staining.

ELISA assay for the plasma and liver

Liver tissues were homogenized and centrifuged at 12000 *g* for 10 min at 4°C in a Sorvall[TM] Legend[TM] Micro 21R Microcentrifuge (Thermo Fisher Scientific). The protein concentration was determined using a Pierce[TM] BCA Protein Assay Kit (Thermo Fisher Scientific; 23225).

The plasma and liver concentrations of the following proteins were measured using the corresponding enzyme-linked immunosorbent assay (ELISA) kit according to the manufacturers' instructions: free fatty acids (FFA; Shanghai Enzyme-linked Biotechnology, Shanghai, China; ml003228-1); aspartate aminotransferase (AST; Nanjing Jiancheng Bioengineering

Institute, Nanjing, China; C010-2-1); alanine aminotransferase (ALT; Nanjing Jiancheng Bioengineering Institute; C009-2-1); superoxide dismutase (SOD; Nanjing Jiancheng Bioengineering Institute; A001-3); glutathione (GSH; Nanjing Jiancheng Bioengineering Institute; A006-2); malondialdehyde (MDA; Nanjing Jiancheng Bioengineering Institute; A003-1); catalase (CAT; Nanjing Jiancheng Bioengineering Institute; A007-1-1); TNF-α (Hangzhou MultiSciences (Lianke) Biotech, Hangzhou, China; 70-EK382/2); and IL-6 (Hangzhou MultiSciences (Lianke) Biotech; 70-EK306/3). The minimum detectable concentrations were 75 μM/l for FFA, 10 U/l for ALT, 10 U/l for AST, 0.05 mg/ml for SOD, 0.5 U/ml for GSH, 0.5 nmol/ml for MDA, 0.5 μmol/ml for CAT, 0.43 pg/ml for TNF-α and 2.75 pg/ml for IL-6. Intra- and interassay coefficients of variation for all ELISAs were < 5% and <8%, respectively.

TUNEL assay

The paraffin-embedded liver samples were cut into 4 μm sections, deparaffinized in xylene and rehydrated through a graded series of ethanol. The apoptotic liver cells were detected using a triphosphate nick-end labelling (TUNEL) assay kit (MK1020 TUNEL Apoptosis Detection Kit-POD (20T); Boster, Pleasanton, CA, USA). After staining with the kit, the sections were counterstained with haematoxylin and then dehydrated and mounted with resin. The apoptotic cells stained brown in the TUNEL assay. All the sections were visualized and photographed using a DM4 M microscope (Leica).

Detection of lipids in the plasma

The plasma concentrations of triglyceride (TG), total cholesterol (CHOL), high-density lipoprotein cholesterol (HDL-C)

and low-density lipoprotein cholesterol (LDL-C) were measured using an automatic electrochemiluminescence immunoassay instrument (Cobas e 602 module; Roche) according to the manufacturer's instructions.

Statistical analyses

All statistical analyses were performed using GraphPad Prism® software (GraphPad Software, San Diego, CA, USA) software. The data are presented as mean ± SD. Student's t-test was used to analyse the data. The number of samples used in each analysis is shown in each figure. A P-value < 0.05 was considered statistically significant.

Results

To investigate the effects of tanshinone IIA treatment on fatty liver disease, the current study established a NAFLD rat model by feeding rats an HFD for 4 months. Control rats were fed a regular diet for 4 months. During the final 2 months, one group of HFD rats received sodium tanshinone II A sulfonate injections once daily (Figure 1a). The mean ± SD body weight in the HFD group was significantly increased compared with the CON group ($P < 0.05$), while the TAN group had a lower mean ± SD body weight than the HFD group (Figure 1b). Plasma concentrations of TG, CHOL and LDL-C were significantly increased in the HFD group compared with the CON group ($P < 0.05$ for all comparisons); and the HDL-C level was significantly decreased in the HFD group compared with the CON group ($P < 0.05$) (Figures 1c–1f). Tanshinone IIA treatment significantly reduced the plasma TG concentration to the CON level and significantly increased the HDL-C level to the CON level ($P < 0.05$ for all comparisons) (Figures 1c and 1e). Although the plasma CHOL and LDL-C levels in the TAN group were significantly higher than those of the CON group ($P < 0.05$ for both comparisons), they were significantly lower than those of the HFD group ($P < 0.05$ for both comparisons) (Figures 1d and 1f). Liver function was examined by measuring plasma levels of ALT and AST (Figure 1g). The significant increases in plasma ALT and AST activities that were induced in the HFD group compared with the CON group ($P < 0.05$ for both comparisons) were significantly attenuated by tanshinone IIA treatment ($P < 0.05$ for both comparisons; TAN group versus HFD group).

When the resected livers were examined macroscopically, the livers from the CON group had a normal shape and appearance, whereas those from the HFD group had the appearance of severe fatty livers and those from the TAN group were mildly fatty livers (Figure 2a). The liver weight and liver/body weight ratio were significantly higher in the TAN group compared with the CON group ($P < 0.05$ for both comparisons), but they were significantly lower compared with the HFD group ($P < 0.05$ for both comparisons) (Figures 2b and 2c). To further examine whether tanshinone IIA treatment abrogates liver weight gain via a reduction in lipid accumulation in the liver, the concentrations of TG, CHOL, FFA, HDL-C and LDL-C in the liver were measured. The liver concentrations of TG, CHOL, FFA and LDL-C in the TAN group were significantly decreased compared with the HFD group ($P < 0.05$ for all comparisons), but the concentrations were significantly higher compared with the CON group ($P < 0.05$ for all comparisons) (Figures 2d–2g). The liver HDL-C concentration in the TAN group was significantly higher compared with the HFD group ($P < 0.05$) and showed a similar level to that of the CON group (Figure 2h).
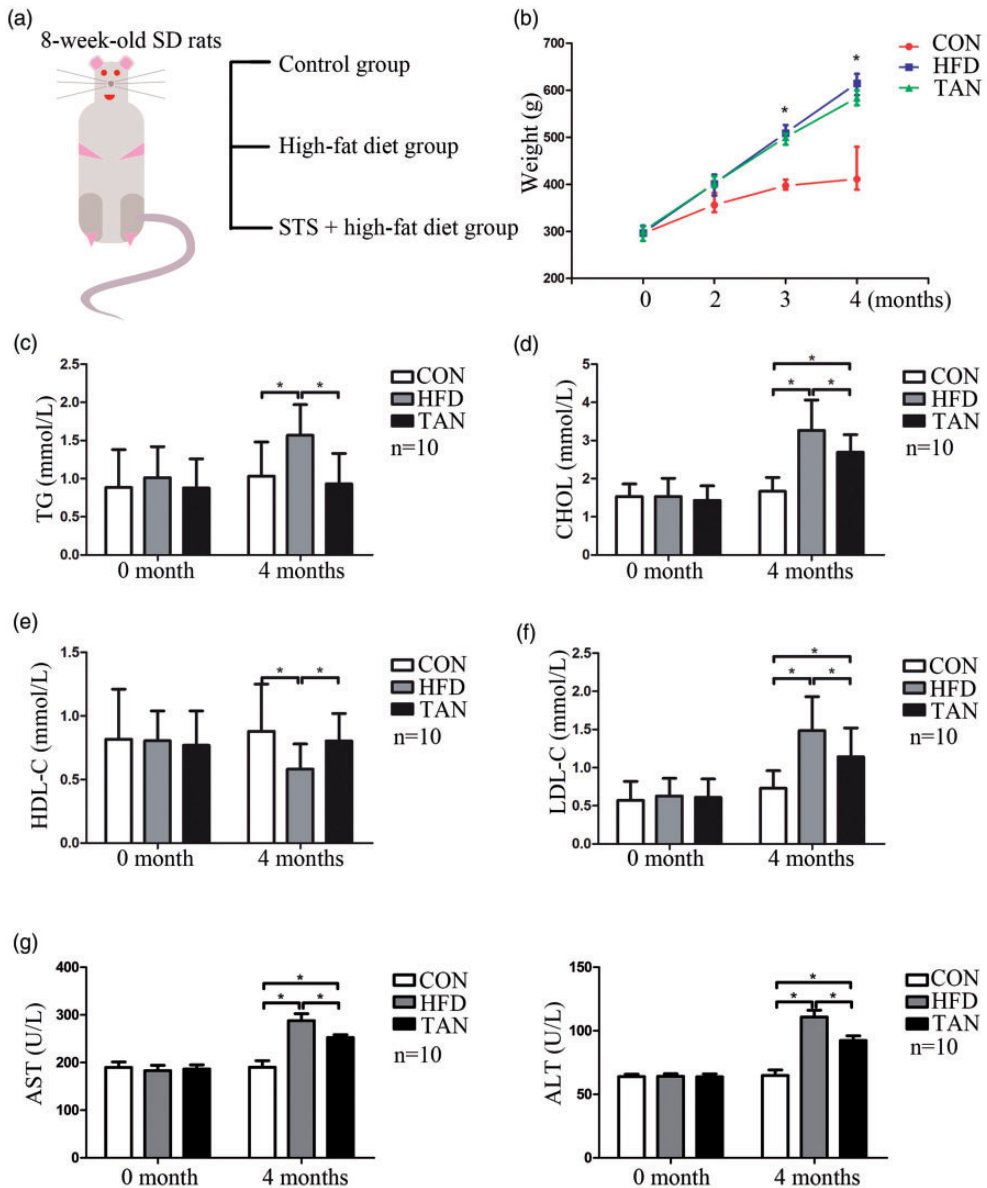
Figure 1. Body weight and plasma concentrations of triglyceride (TG), total cholesterol (CHOL), high-density lipoprotein cholesterol (HDL-C), low-density lipoprotein cholesterol (LDL-C), aspartate amino-transferase (AST) and alanine aminotransferase (ALT) of rats in the three study groups. (a) Eight-week-old male Sprague Dawley (SD) rats were randomly assigned to one of three groups: control group (CON; normal feed for 4 months); high-fat diet group (HFD for 4 months); and 2 months of HFD followed by 2 months treatment with 10 mg/kg sodium tanshinone IIA sulfonate (STS) once daily plus HFD (TAN) group ($n = 10$ rats per group); (b) Changes in the mean $\pm$ SD body weight in the three groups over the 4-month study period; *$P < 0.05$ for HFD versus TAN; Student's t-test; (c) Mean $\pm$ SD plasma TG levels in the three groups; (d) Mean $\pm$ SD plasma CHOL levels in the three groups; (e) Mean $\pm$ SD plasma HDL-C levels in the three groups; (f) Mean $\pm$ SD plasma LDL-C levels in the three groups; (g) Mean $\pm$ SD plasma levels of ALT and AST in the three groups. TG, triglycerides. *$P < 0.05$, Student's t-test.
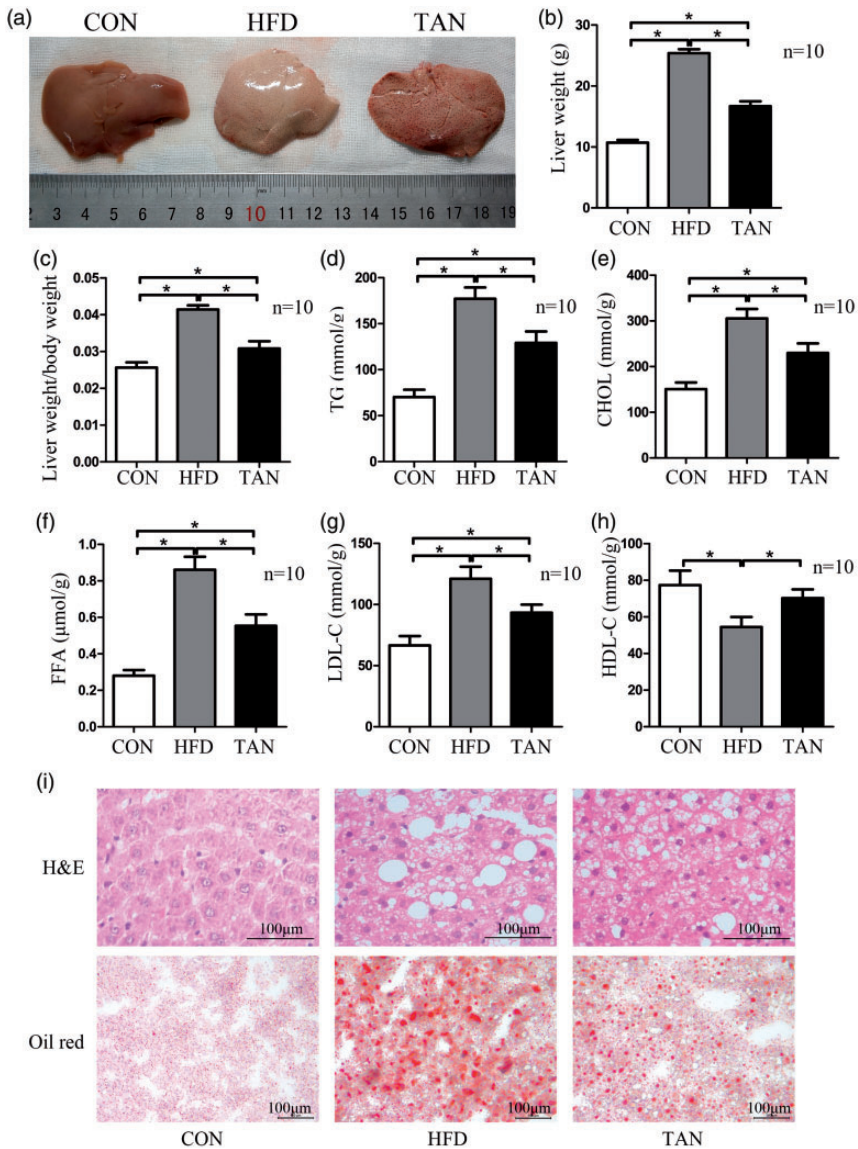
Figure 2. Liver weights, liver lipid accumulation and liver concentrations of triglyceride (TG), total cholesterol (CHOL), free fatty acids (FFA), high-density lipoprotein cholesterol (HDL-C) and low-density lipoprotein cholesterol (LDL-C) of rats in the three study groups: CON (normal feed for 4 months); high-fat diet group (HFD for 4 months); and 2 months of HFD followed by 2 months treatment with 10 mg/kg sodium tanshinone IIA sulfonate once daily plus HFD (TAN) group ($n = 10$ rats per group). (a) Photographic images of whole livers from representative rats from each of the three study groups; (b) Liver weight in the three groups at the end of the 4-month study. Data presented as mean $\pm$ SD. *$P < 0.05$, Student's t-test.; (c) Liver weight/body weight ratio in the three groups at the end of the 4-month study; (d–h) TG, CHOL, FFA, LDL-C and HDL-C levels in liver tissue homogenate as measured using enzyme-linked immunosorbent assay kits. Data presented as mean $\pm$ SD. *$P < 0.05$, Student's t-test; (i) Haematoxylin and eosin (h&e) and oil red-O staining of liver sections from the CON, HFD and TAN groups. Scale bar 100 μm. The colour version of this figure is available at: http://imr.sagepub.com.

Microscopic observations of the liver sections stained with haematoxylin and eosin showed normal liver morphology in the CON group (Figure 2i). The livers of the rats in the HFD group showed hepatic steatosis with accumulation of triglyceride inside hepatocytes. The affected hepatocytes showed typical single or multiple lipid droplets within the cytoplasm, which displaced the nucleus to the periphery of the cell. In the TAN group, the hepatic lipid accumulation was visibly reduced compared with the HFD group. Oil red-O staining was used to further investigate if lipid accumulation was decreased by tanshinone IIA treatment. The livers in the rats in the HFD group showed very large lipid droplets, suggesting potential liver damage. In the TAN group, the number and size of the lipid droplets were reduced compared with the HFD group.

Previous research demonstrated that activation of TLR4 modulates the inflammatory response that contributes to the pathogenesis of NAFLD.[11] The current study investigated the role of the TLR4 pathway in mediating the effects of tanshinone IIA treatment on fatty liver disease. In the TAN group, the mRNA levels of TLR4, MyD88, NF-κB and Ikk-β were all significantly lower than those of the HFD group ($P < 0.05$ for all comparisons) (Figures 3a–3d). Similar findings were observed for the protein levels of TLR4, MyD88, NF-κB and Ikk-β as measured by Western blot analysis in the TAN group compared with the HFD group ($P < 0.05$ for all comparisons) (Figures 3e and 3f). To examine the activity of NF-κB, the levels of p-NF-κB protein in the nucleus were measured using Western blot analysis. NF-κB was activated in the HFD group, while tanshinone IIA treatment significantly reduced the levels of nuclear p-NF-κB protein compared with the HFD group ($P < 0.05$) (Figures 3e and 3f). To verify that the NF-κB activity was decreased by

tanshinone IIA treatment, the levels of Ikk-β and p-IκB-α proteins were measured using Western blot analysis. Tanshinone IIA treatment significantly reduced the levels of Ikk-β and p-IκB-α protein compared with the HFD group ($P < 0.05$ for both comparisons) (Figures 3e and 3f). The protein levels of Ikk-β and p-IκB-α were significantly upregulated in the HFD group compared with the CON group ($P < 0.05$ for both comparisons).

Triphosphate nick-end labelling was used to investigate whether TLR4 downregulated by tanshinone IIA treatment could reduce apoptosis in fatty liver disease (Figure 3g). Apoptotic cells can be observed in the HFD group (arrows in Figure 3g), while very few were visualized in the TAN group. The plasma protein levels of IL-6, TNF-α and IL-1β, which are downstream of TLR4/MyD88/NF-κB, were measured using ELISA kits (Figure 3h). The plasma IL-6, TNF-α and IL-1β protein levels in the TAN group were significantly reduced compared with the HFD group ($P < 0.05$ for all comparisons), although the levels remained higher than the CON group.

The current study investigated the levels of PPAR-γ in the liver because it has been previously reported to be involved in the development of fatty liver disease.[10,39] PPAR-γ mRNA levels were significantly upregulated in the HFD group compared with the CON group ($P < 0.05$), while PPAR-γ protein levels in whole cell and nuclear lysates showed small increases in the HFD group compared with the CON group (Figures 4a–4c). The levels of PPAR-γ mRNA and protein in whole cell and nuclear lysates in the TAN group were significantly higher compared with the HFD group by real-time PCR and Western blot analysis ($P < 0.05$ for all comparisons). PGC-1α protein levels were upregulated by tanshinone IIA treatment compared with the HFD group (Figure 4c).
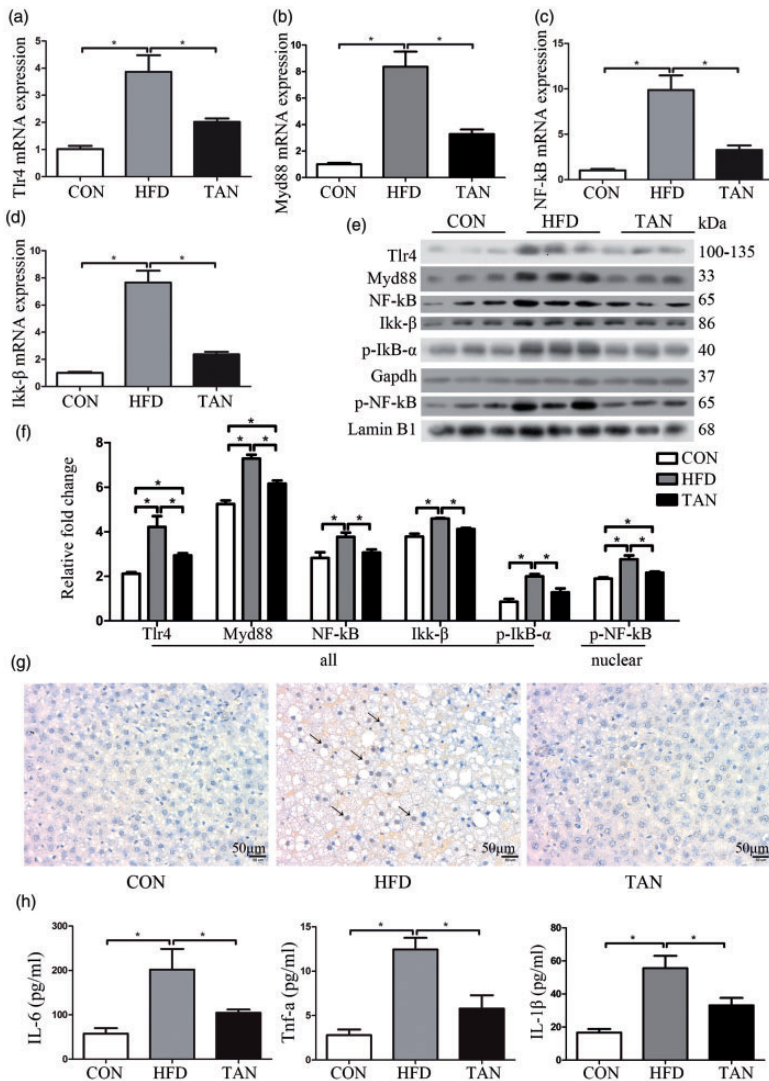
Figure 3. Protein and mRNA levels of components of the toll-like receptor 4 (TLR4)/nuclear factor kappa B (NF-κB) signalling pathway, levels of liver cell apoptosis and plasma concentrations of interleukin (IL)-6, tumour necrosis factor (TNF)-α and IL-1β in the three study groups: CON (normal feed for 4 months); high-fat diet group (HFD for 4 months); and 2 months of HFD followed by 2 months treatment with 10 mg/kg sodium tanshinone IIA sulfonate once daily plus HFD (TAN) group (n = 10 rats per group). TLR4 mRNA levels (a), myeloid differentiation primary response 88 (MyD88) mRNA levels (b), NF-κB mRNA levels (c) and IkB kinase (Ikk-β) mRNA levels (d) were detected by real-time polymerase chain reaction; (e) Western blot analysis to measure levels of TLR4, MyD88, NF-κB, Ikk-β, phospho (p)-IκB-α and phospho (p)-NF-κB (nuclear) proteins in the three study groups. Glyceraldehyde 3-phosphate dehydrogenase (GAPDH) was the internal loading control and lamin B1 was the nuclear control; (e) Relative levels of each protein according to the Western blot results; (g) Triphosphate nick-end labelling of apoptotic cells in liver sections from the three study groups. Apoptotic cells (arrows). Scale bar 50 μm; (h) Plasma concentrations of IL-6, TNF-α and IL-1β in the three study groups as measured using enzyme-linked immunosorbent assay kits. Data presented as mean ± SD. *P < 0.05, Student's t-test. kDa, kilodalton. The colour version of this figure is available at: http://imr.sagepub.com.
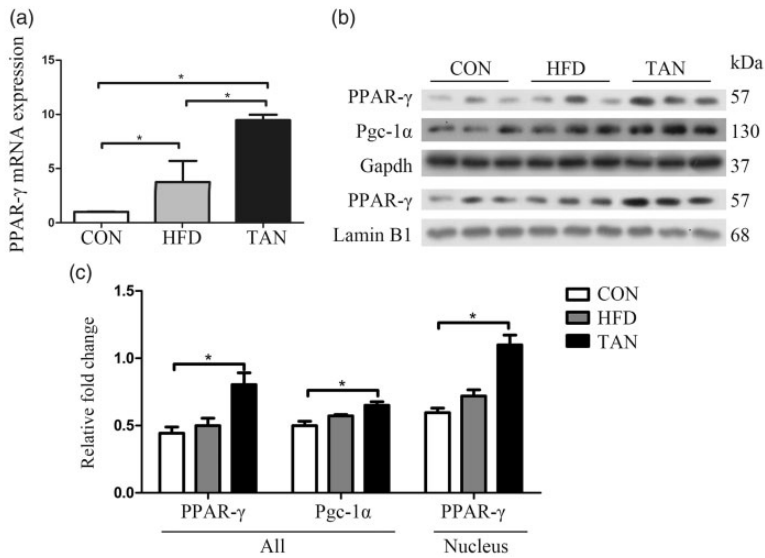
Figure 4. Protein and mRNA levels of peroxisome proliferator-activated receptor gamma (PPAR-γ) and peroxisome proliferator-activated receptor gamma coactivator-1 alpha (PGC-1α) in the three study groups: CON (normal feed for 4 months); high-fat diet group (HFD for 4 months); and 2 months of HFD followed by 2 months treatment with 10 mg/kg sodium tanshinone IIA sulfonate once daily plus HFD (TAN) group ($n = 10$ rats per group). (a) PPAR-γ mRNA levels were detected by real-time polymerase chain reaction; (b) Western blot analysis to measure levels of PPAR-γ and PGC-1α proteins in the three study groups. Glyceraldehyde 3-phosphate dehydrogenase (GAPDH) was the internal loading control and lamin B1 was the nuclear control; (c) Relative levels of each protein according to the Western blot results. Data presented as mean $\pm$ SD. *$P < 0.05$, Student's t-test. kDa, kilodalton.

As PPAR-γ is implicated in the oxidative stress response,[40,41] this current study measured the levels of the oxidative stress markers, SOD, GSH and MDA, in plasma and liver tissue homogenate from rats in the three study groups using ELISA kits. The levels of SOD protein in the plasma and liver tissues were low in the HFD group but were significantly increased by tanshinone IIA treatment ($P < 0.05$ for both comparisons; TAN group versus HFD group) (Figures 5a and 5b). Although tanshinone IIA treatment significantly increased the GSH level in the plasma and liver tissues compared with the HFD group ($P < 0.05$ for both comparisons), the GSH concentrations in the TAN group remained lower compared with the CON group ($P < 0.05$ for plasma only) (Figures 5a and 5b).

The MDA levels in the plasma and liver tissues were significantly increased in the HFD group compared with the CON group ($P < 0.05$ for both comparisons) and tanshinone IIA treatment significantly reduced the levels back to CON levels ($P < 0.05$ for both comparisons; TAN group versus HFD group) (Figures 5a and 5b). To further investigate the effect of tanshinone IIA treatment on oxidative stress, the CAT concentration in the liver tissue homogenate from rats in the three study groups was determined using an ELISA kit. CAT activity was significantly decreased in the HFD group compared with the CON group ($P < 0.05$); and tanshinone IIA treatment significantly increased the CAT activity compared with the HFD group ($P < 0.05$; TAN group versus HFD group) (Figure 5c).
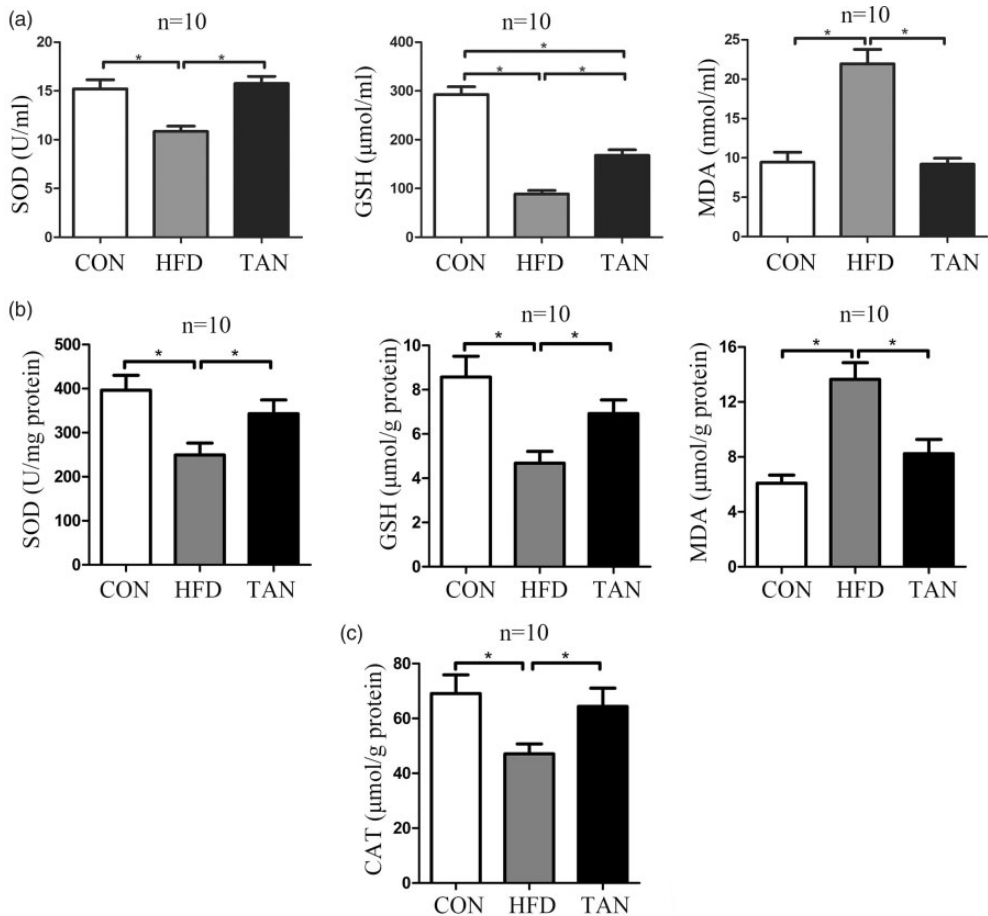
Figure 5. Oxidative status in the plasma and liver was determined by measuring superoxide dismutase (SOD), glutathione peroxidase (GSH), malondialdehyde (MDA) and catalase (CAT) protein levels using enzyme-linked immunosorbent assay kits in the three study groups: CON (normal feed for 4 months); high-fat diet group (HFD for 4 months); and 2 months of HFD followed by 2 months treatment with 10 mg/kg sodium tanshinone IIA sulfonate once daily plus HFD (TAN) group ($n = 10$ rats per group). (a) plasma levels; (b) levels in liver tissue homogenate; (c) CAT levels in liver tissue homogenate. Data presented as mean $\pm$ SD. *$P < 0.05$, Student's t-test.

Discussion

There is a lack of approved therapies for NAFLD despite the prevalence being high and the incidence increasing.[42] Currently, the mainstay of treatment for NAFLD is weight loss, but this is hard to maintain in the long term.[43] There is considerable need for novel pharmacotherapeutic agents for NAFLD. Tanshinone IIA has anti-atherosclerosis, anti-cardiac hypertrophy, anti-oxidant, anti-arrhythmia and anti-inflammatory properties.[32,33] Known as Danshen, it is widely used to treat cardiovascular and cerebrovascular diseases following adverse treatment effects in China.[34] However, its role as a potential treatment for NAFLD has not been extensively studied.[44,45]

This current study has provided evidence for the role of tanshinone IIA in hepatic steatosis. A plasma-lipid signature, which had a sensitivity of 69.1% and specificity of 73.8% for NAFLD diagnosis, was developed to estimate the percentage of liver fat.[46] This current study demonstrated that tanshinone IIA treatment reduced plasma and liver lipid levels, liver weight and increased the levels of the liver function markers ALT and AST, suggesting that this drug may protect against hepatic steatosis. Previous research has demonstrated that tanshinone IIA can reduce adipose mass and body weight without changing the food intake in an HFD model,[47] suggesting that the effects of tanshinone IIA on adipose and body weight reductions are not due to decreased food intake.

Recent research has shown that TLR4 mutant mice are resistant to NAFLD.[26,48,49] More importantly, TLR4 signalling is a key pathway involved in the progression of NAFLD in humans.[11] The activity of NF-κB is closely mediated by interactions with IκBs and it has been reported that IκB-α makes multiple contacts with NF-κB.[15] Normally, the NF-κB–IκB complex is inactive in the cytoplasm.[15] Ikk, regulated by MyD88, is called NF-κB essential modulator (NEMO) because it mediates phosphorylation of IκB that induces degradation.[15,16] In this current study, the protein levels of TLR4, MyD88, Ikk-β, p-IκB-α and nuclear p-NF-κB were significantly reduced by tanshinone IIA treatment compared with the HFD group, suggesting that activation of the TLR4/MyD88/Ikk-β/IκB-α/NF-κB signalling pathway was reduced by tanshinone IIA. As an integrator of the inflammatory pathway, activation of NF-κB regulates pro-inflammatory cytokines, such as IL-6 and TNF-α in NAFLD.[50] Treatment with tanshinone IIA decreased IL-6 and TNF-α levels in plasma compared with the HFD group. Moreover, activation of NF-κB can increase pro-IL-1β.[29] Activation of IL-1β by caspase 1 not only promotes recruitment of inflammatory cells to the liver, but it also induces triglyceride accumulation in liver.[29] It has been reported that the TLR4/NF-κB signalling pathway is involved in cell apoptosis.[51] In addition, IL-1β induced by TLR4/NF-κB signalling can trigger hepatocyte death in conjunction with TNF.[29] Combined with inhibition of cell apoptosis in the liver in the TAN group, these current findings suggest that tanshinone IIA inhibits apoptosis via the downregulation of the TLR4/NF-κB/IL-1β signalling pathway. In our opinion, tanshinone IIA inactivates the TLR4/NF-κB signalling pathway, which in turn results in a reduction of inflammatory mediators in the plasma and inhibition of liver cell apoptosis.

Peroxisome proliferator-activated receptor gamma, a master transcriptional regulator of adipogenesis, contributes to the process of lipid storage.[52] The increasing levels of PPAR-γ in fatty liver promotes hepatic lipid accumulation.[53] Not only the upregulation of PPAR-γ, but also treatment with the PPAR-γ agonist rosiglitazone can reduce the progression of fatty liver disease.[52] The protective effects of PPAR-γ may be due to increased insulin sensitivity in adipose tissue and protection against oxidative stress.[41,52] Tanshinone IIA can modify the transcriptional activities of PPAR-γ in liver tissues in an HFD animal model.[47] In this current study, treatment with tanshinone IIA increased the levels of PGC-1α protein in whole cell lysates and PPAR-γ protein levels in both whole cell and nuclear lysates, thus ameliorating the oxidative stress in rats fed an HFD. These current results suggest that tanshinone IIA prevents the development of fatty liver disease through upregulation of PPAR-γ leading to amelioration of oxidative stress.

A better understanding of disease pathogenesis is often followed by the

development of new classes of medications.[42] Innovative therapeutic targets for NAFLD include four main pathways: hepatic fat accumulation; oxidative stress, inflammation and apoptosis; intestinal microbiomes; and metabolic endotoxaemia and hepatic fibrosis.[42] The HFD rat model is a common model used to study NAFLD. Research has demonstrated that tanshinone IIA reduced fatty liver accumulation through suppression of lipogenesis and inflammation by activation of the sirtuin 1/protein kinase adenosine monophospate-activated catalytic subunit alpha 1 pathway.[45] In this current research, the HFD rat model was used to investigate the effect of tanshinone IIA on NAFLD.

In conclusion, tanshinone IIA reduced fat accumulation in the liver and reduced plasma lipid levels in an HFD rat model. It also partly ameliorated oxidative stress, inflammation and apoptosis in NAFLD by targeting TLR4 and PPAR-γ. This current study also demonstrated that tanshinone IIA stimulated PPAR-γ and downregulated TLR4, which protected rats fed an HFD against fatty liver disease. These current findings provide a novel framework of tanshinone IIA function on fatty liver accumulation that should facilitate the development of NAFLD therapies in the future.

Declaration of conflicting interest

The authors declare that there are no conflicts of interest.

Funding

ORCID iD

Lu Huang   https://orcid.org/0000-0003-2219-7134

References

1. Brunt EM, Wong VW, Nobili V, et al. Nonalcoholic fatty liver disease. *Nat Rev Dis Primers* 2015; 1: 15080.
2. Marchesini G, Petta S and Dalle Grave R. Diet, weight loss, and liver health in nonalcoholic fatty liver disease: pathophysiology, evidence, and practice. *Hepatology* 2016; 63: 2032–2043.
3. Said A and Ghufran A. Epidemic of nonalcoholic fatty liver disease and hepatocellular carcinoma. *World J Clin Oncol* 2017; 8: 429–436.
4. Khan R, Bril F, Cusi K, et al. Modulation of insulin resistance in NAFLD. *Hepatology* 2018. doi: 10.1002/hep.30429.
5. Kohli R, Boyd T, Lake K, et al. Rapid progression of NASH in childhood. *J Pediatr Gastroenterol Nutr* 2010; 50: 453–456.
6. Sass DA, Chang P and Chopra KB. Nonalcoholic fatty liver disease: a clinical review. *Dig Dis Sci* 2005; 50: 171–180.
7. Forman BM, Tontonoz P, Chen J, et al. 15-Deoxy-delta 12, 14-prostaglandin J2 is a ligand for the adipocyte determination factor PPAR gamma. *Cell* 1995; 83: 803–812.
8. Kliewer SA, Lenhard JM, Willson TM, et al. A prostaglandin J2 metabolite binds peroxisome proliferator-activated receptor gamma and promotes adipocyte differentiation. *Cell* 1995; 83: 813–819.
9. Nierenberg AA, Ghaznavi SA, Sande Mathias I, et al. Peroxisome proliferator-activated receptor gamma coactivator-1 alpha as a novel target for bipolar disorder and other neuropsychiatric disorders. *Biol Psychiatry* 2018; 83: 761–769.
10. Vidal-Puig A, Jimenez-Linan M, Lowell BB, et al. Regulation of PPAR gamma gene expression by nutrition and obesity in rodents. *J Clin Invest* 1996; 97: 2553–2561.
11. Miura K and Ohnishi H. Role of gut microbiota and Toll-like receptors in nonalcoholic fatty liver disease. *World J Gastroenterol* 2014; 20: 7381–7391.

12. Alexopoulou L, Holt AC, Medzhitov R, et al. Recognition of double-stranded RNA and activation of NF-kappaB by Toll-like receptor 3. *Nature* 2001; 413: 732–738.

13. Imajo K, Fujita K, Yoneda M, et al. Hyperresponsivity to low-dose endotoxin during progression to nonalcoholic steatohepatitis is regulated by leptin-mediated signaling. *Cell Metab* 2012; 16: 44–54.

14. Jefferies CA and O'Neill LA. Bruton's tyrosine kinase (Btk)-the critical tyrosine kinase in LPS signalling? *Immunol Lett* 2004; 92: 15–22.

15. Gilmore TD. Introduction to NF-kappaB: players, pathways, perspectives. *Oncogene* 2006; 25: 6680–6684.

16. Yang Y, Lv J, Jiang S, et al. The emerging role of Toll-like receptor 4 in myocardial inflammation. *Cell Death Dis* 2016; 7: e2234.

17. Tong Y, Cui J, Li Q, et al. Enhanced TLR-induced NF-kappaB signaling and type I interferon responses in NLRC5 deficient mice. *Cell Res* 2012; 22: 822–835.

18. Williams KJ, Brocia RW and Fisher EA. The unstirred water layer as a site of control of apolipoprotein B secretion. *J Biol Chem* 1990; 265: 16741–16744.

19. Silk E, Zhao H, Weng H, et al. The role of extracellular histone in organ injury. *Cell Death Dis* 2017; 8: e2812.

20. Paik YH, Schwabe RF, Bataller R, et al. Toll-like receptor 4 mediates inflammatory signaling by bacterial lipopolysaccharide in human hepatic stellate cells. *Hepatology* 2003; 37: 1043–1055.

21. Marinovic MP, Morandi AC and Otton R. Green tea catechins alone or in combination alter functional parameters of human neutrophils via suppressing the activation of TLR-4/NFkappaB p65 signal pathway. *Toxicol In Vitro* 2015; 29: 1766–1778.

22. Xia X, Cui J, Wang HY, et al. NLRX1 negatively regulates TLR-induced NF-kappaB signaling by targeting TRAF6 and IKK. *Immunity* 2011; 34: 843–853.

23. Ye D, Li FY, Lam KS, et al. Toll-like receptor-4 mediates obesity-induced non-alcoholic steatohepatitis through activation of X-box binding protein-1 in mice. *Gut* 2012; 61: 1058–1067.

24. Liu H, Li J, Tillman B, et al. TLR3/4 signaling is mediated via the NFκB-CXCR4/7 pathway in human alcoholic hepatitis and non-alcoholic steatohepatitis which formed Mallory-Denk bodies. *Exp Mol Pathol* 2014; 97: 234–240.

25. Wang YL, Liu LJ, Zhao WH, et al. Intervening TNF-α via PPARγ with gegenqinlian decoction in experimental nonalcoholic fatty liver disease. *Evid Based Complement Alternat Med* 2015; 2015: 715638.

26. Rivera CA, Adegboyega P, van Rooijen N, et al. Toll-like receptor-4 signaling and Kupffer cells play pivotal roles in the pathogenesis of non-alcoholic steatohepatitis. *J Hepatol* 2007; 47: 571–579.

27. Gao Y, Chen X, Fang L, et al. Rhein exerts pro- and anti-inflammatory actions by targeting IKKβ inhibition in LPS-activated macrophages. *Free Radic Biol Med* 2014; 72: 104–112.

28. Kugelmas M, Hill DB, Vivian B, et al. Cytokines and NASH: a pilot study of the effects of lifestyle modification and vitamin E. *Hepatology* 2003; 38: 413–419.

29. Szabo G and Petrasek J. Inflammasome activation and function in liver disease. *Nat Rev Gastroenterol Hepatol* 2015; 12: 387–400.

30. Bai L and Li H. Innate immune regulatory networks in hepatic lipid metabolism. *J Mol Med (Berl)* 2019; 97: 593–604.

31. Li D, Wang J, Sun D, et al. Tanshinone IIA sulfonate protects against cigarette smoke-induced COPD and down-regulation of CFTR in mice. *Sci Rep* 2018; 8: 376.

32. Chen FY, Guo R and Zhang BK. Advances in cardiovascular effects of tanshinone II(A). *Zhongguo Zhong Yao Za Zhi* 2015; 40: 1649–1653 [Article in Chinese, English abstract].

33. Jia PT, Zhang XL, Zuo HN, et al. Articular cartilage degradation is prevented by tanshinone IIA through inhibiting apoptosis and the expression of inflammatory cytokines. *Mol Med Rep* 2017; 16: 6285–6289.

34. Zhou L, Zuo Z and Chow MS. Danshen: an overview of its chemistry, pharmacology, pharmacokinetics, and clinical use. *J Clin Pharmacol* 2005; 45: 1345–1359.

35. Wei Y, Gao J, Qin L, et al. Tanshinone I alleviates insulin resistance in type 2 diabetes

mellitus rats through IRS-1 pathway. *Biomed Pharmacother* 2017; 93: 352–358.

36. Li J, Zheng Y, Li MX, et al. Tanshinone IIA alleviates lipopolysaccharide-induced acute lung injury by downregulating TRPM7 and pro-inflammatory factors. *J Cell Mol Med* 2018; 22: 646–654.

37. Yang GL, Jia LQ, Wu J, et al. Effect of tanshinone IIA on oxidative stress and apoptosis in a rat model of fatty liver. *Exp Ther Med* 2017; 14: 4639–4646.

38. Li SY, Yan JQ, Song Z, et al. Molecular characterization of lysyl oxidase-mediated extracellular matrix remodeling during mouse decidualization. *FEBS Lett* 2017; 591: 1394–1407.

39. Rahimian R, Masih-Khan E, Lo M, et al. Hepatic over-expression of peroxisome proliferator activated receptor gamma2 in the ob/ob mouse model of non-insulin dependent diabetes mellitus. *Mol Cell Biochem* 2001; 224: 29–37.

40. Polvani S, Tarocchi M and Galli A. PPARγ and Oxidative Stress: Con(β) Catenating NRF2 and FOXO. *PPAR Res* 2012; 2012: 641087.

41. Chan SH, Wu KL, Kung PS, et al. Oral intake of rosiglitazone promotes a central antihypertensive effect via upregulation of peroxisome proliferator-activated receptor-gamma and alleviation of oxidative stress in rostral ventrolateral medulla of spontaneously hypertensive rats. *Hypertension* 2010; 55: 1444–1453.

42. Rotman Y and Sanyal AJ. Current and upcoming pharmacotherapy for nonalcoholic fatty liver disease. *Gut* 2017; 66: 180–190.

43. Sweet PH, Khoo T and Nguyen S. Nonalcoholic fatty liver disease. *Prim Care* 2017; 44: 599–607.

44. Song HY, Zhang L, Pan JL, et al. Bioactivity of five components of Chinese herbal formula Jiangzhi granules against hepatocellular steatosis. *J Integr Med* 2013; 11: 262–268.

45. Li XX, Lu XY, Zhang SJ, et al. Sodium tanshinone IIA sulfonate ameliorates hepatic steatosis by inhibiting lipogenesis and inflammation. *Biomed Pharmacother* 2019; 111: 68–75.

46. Oresic M, Hyotylainen T, Kotronen A, et al. Prediction of non-alcoholic fatty-liver disease and liver fat content by plasma molecular lipids. *Diabetologia* 2013; 56: 2266–2274.

47. Gong Z, Huang C, Sheng X, et al. The role of tanshinone IIA in the treatment of obesity through peroxisome proliferator-activated receptor gamma antagonism. *Endocrinology* 2009; 150: 104–113.

48. Csak T, Velayudham A, Hritz I, et al. Deficiency in myeloid differentiation factor-2 and toll-like receptor 4 expression attenuates nonalcoholic steatohepatitis and fibrosis in mice. *Am J Physiol Gastrointest Liver Physiol* 2011; 300: G433–G441.

49. Poggi M, Bastelica D, Gual P, et al. C3H/HeJ mice carrying a toll-like receptor 4 mutation are protected against the development of insulin resistance in white adipose tissue in response to a high-fat diet. *Diabetologia* 2007; 50: 1267–1276.

50. Chen Z, Yu R, Xiong Y, et al. A vicious circle between insulin resistance and inflammation in nonalcoholic fatty liver disease. *Lipids Health Dis*. 2017; 16: 203.

51. Liang C, Wang X, Hu J, et al. PTPRO promotes oxidized low-density lipoprotein induced oxidative stress and cell apoptosis through toll-like receptor 4/nuclear factor κB pathway. *Cell Physiol Biochem* 2017; 42: 495–505.

52. Huang YY, Gusdon AM and Qu S. Nonalcoholic fatty liver disease: molecular pathways and therapeutic strategies. *Lipids Health Dis* 2013; 12: 171.

53. Lee YJ, Ko EH, Kim JE, et al. Nuclear receptor PPARγ-regulated monoacylglycerol O-acyltransferase 1 (MGAT1) expression is responsible for the lipid accumulation in diet-induced hepatic steatosis. *Proc Natl Acad Sci U S A* 2012; 109: 13656–13661.